Atmospheric
Chemistry
and Physics
Discussions

Open Access

Natural new particle formation at the coastal Antarctic site Neumayer

R. Weller[1], K. Schmidt[1], K. Teinilä[2], and R. Hillamo[2]

[1]Alfred Wegener Institute for Polar and Marine Research, Am Handelshafen 12, 27570 Bremerhaven, Germany
[2]Finnish Meteorological Institute, Erik Palménin aukio 1, 00101 Helsinki, Finland

Correspondence to: R. Weller (rolf.weller@awi.de)

Discussion Paper | Discussion Paper | Discussion Paper | Discussion Paper

ACPD

15, 15655–15681, 2015

Natural new particle formation

R. Weller et al.

Title Page

Abstract	Introduction
Conclusions	References
Tables	Figures

|◄ ►|

◄ ►

Back Close

Full Screen / Esc

Printer-friendly Version

Interactive Discussion

Abstract

We measured condensation particle (CP) concentrations and particle size distributions at the coastal Antarctic station Neumayer ($70°39'$ S, $8°15'$ W) during two summer campaigns (from 20 January to 26 March 2012 and 1 February to 30 April 2014) and during

5   polar night between 12 August and 27 September 2014 in the particle diameter (D_p) range from 2.94 to 60.4 nm (2012) and from 6.26 to 212.9 nm (2014). During both summer campaigns we identified all in all 44 new particle formation (NPF) events. From 10 NPF events, particle growth rates could be determined to be around 0.90 ± 0.46 nm h^{-1} (mean $\pm$ SD; range: 0.4 to 1.9 nm h^{-1}). With the exception of one case, particle growth

10   was generally restricted to the nucleation mode ($D_p < 25$ nm) and the duration of NPF events was typically around 6.0 ± 1.5 h (mean $\pm$ SD; range: 4 to 9 h). Thus in the main, particles did not grow up to sizes required for acting as cloud condensation nuclei. NPF during summer usually occurred in the afternoon in coherence with local photochemistry. During winter, two NPF events could be detected, though showing no ascertain-

15   able particle growth. A simple estimation indicated that apart from sulfuric acid, the derived growth rates required other low volatile precursor vapours.

1   Introduction

The crucial role of aerosols as a key component in governing radiation transfer through the Earth's atmosphere and thus their pivotal role in determining climate, has boosted

20   aerosol research activities and strongly promoted our knowledge on this topic. The decisive role of aerosols in radiative forcing is even amplified since they potentially act as condensation nuclei for cloud droplets, thus influencing radiation transfer indirectly (Haywood and Boucher, 2000; Ramanathan et al., 2001; Carslaw et al., 2013; Rosenfeld et al., 2014). In particular due to the latter effect, involving inherently complicated

25   feedback mechanisms, aerosols still notoriously contribute to the largest uncertainty in estimating climate forcing (for a comprehensive treatise we refer to Boucher et al.,

2013 and references therein). One focus of interest in aerosol research is dedicated to questions regarding new particle formation (NPF), the dominant global particle source generating so-called secondary aerosol (Spracklen et al., 2006). This process starts with the nucleation of gaseous precursors to molecular clusters (Zhang et al., 2012) followed by particle growth to sizes potentially relevant for acting as cloud condensation nuclei (CCN; Spracklen et al., 2008; Bzdek and Johnston, 2010).

Concerning the marine troposphere, recent research activities documented the global importance of natural secondary aerosol and revealed that apart from dimethyl sulfide (DMS) derived sulfuric acid (H_2SO_4), especially marine volatile organic compounds (VOC) but also reactive iodine species mediate particle nucleation and growth (O'Dowd et al., 2002a, b; Henze and Seinfeld, 2006; O'Dowd and de Leeuw, 2007; Facchini et al., 2008a; McFiggans et al., 2010). Notably in terms of secondary aerosol formation, the virtually completely ice covered and thus effectively source free Antarctic continent represents an outstanding case: surrounded and isolated by the Southern Ocean from other continents, NPF should be inherently linked with the advection of marine air masses. Apart from some earlier work reporting on the frequent occurrence of bimodal particle size distributions below 100 nm in coastal Antarctica (Ito, 1985, 1993; Jaenicke et al., 1992), NPF has been recently described for several Antarctic sites. Most extensive measurements were conducted at the Finnish station Aboa (73°03′ S, 13°25′ W, 496 m a.s.l.), located on a nunatuk about 130 km from the sea (Koponen et al., 2003; Asmi et al., 2010; Kyrö et al., 2013). Asmi et al. (2010) reported on NPF events showing growth rates (GR) within the nucleation mode between 0.8 and 2.5 nm h^{-1}, while in a subsequent summer campaign, significantly higher GR between 1.8 and 8.8 nm h^{-1} were found and particle growth usually extended well into the Aitken mode (Kyrö et al., 2013). A thorough data analysis by Kyrö et al. (2013) revealed that most probably biogenic precursors originating from local melting ponds provided low volatile vapour needed for the observed particle growth. Hence this study was the first one indicating that (biogenic) emissions from continental Antarctic could be a source for secondary aerosol formation and relativized the source free charac-

ter of continental Antarctica. Regarding the Antarctic Plateau, NPF events reported from South Pole were ascribed to local contamination (Park et al., 2004). In contrast, during year-round measurements at Dome C (75°06′ S, 123°23′ E, 3200 m a.s.l.) several NPF events could be observed throughout the year, mostly associated with particle growth starting from the nucleation into the Aitken mode (Järvinen et al., 2013). Most surprisingly, growth rates tentatively appeared even higher compared to Aboa (median considering all events: 2.5 nm h^{-1}, range: 0.5 to 14.1 nm h^{-1}; Järvinen et al., 2013). Complementary to these local field investigations, dedicated modelling studies can give spatially inclusive and comprehensive insights regarding sources and mechanisms of NPF and the influence on CCN concentrations in the remote atmosphere of the Southern Ocean. Korhonen et al.'s (2008) work revealed a weaker impact of DMS derived secondary aerosol on marine CCN concentrations at high southern latitudes, largely caused by much stronger sea spray emissions south of 45° S. This study also emphasized the importance of NPF in the free troposphere followed by particle growth during entrainment into the marine boundary layer. Yu and Luo's (2010) investigations targeted on modelling DMS derived NPF around coastal Antarctica and demonstrated that ion-mediated nucleation can reasonably predict the observed seasonality of condensation particle (CP) concentrations at coastal Antarctica.

Our present work ties in with a previous publication that examined the climatology of CP concentrations at the German Antarctic research station Neumayer (Weller et al., 2011a). This precedent study indicated the importance of particle nucleation occurring even during late winter and early spring in determining particle number concentrations. In the current study we will entirely focus on the dynamics of particle size distribution and NPF, relying on two dedicated summer campaigns in 2012 and 2014, as well as a measuring period during austral winter (August and September 2014).

2 Experimental techniques and data evaluation methods

2.1 Site description and instrumentation

All experiments were conducted inside the Air Chemistry Observatory located close to Neumayer Station (NM, 70°39′ S, 8°15′ W, http://www.awi.de/en/go/air_chemistry_observatory, last access: 24 March 2015). Measuring site, prevailing local meteorological conditions, characteristics of the air inlet system, and finally aspects of contamination free sampling have already been described in some detail and we refer to König-Langlo et al. (1998) and Weller et al. (2011a, and references therein).

The size distribution of the sub-µm aerosol at NM was determined by a scanning mobility particle sizer (SMPS, TSI classifier model 3080; Wang and Flagan, 1990). During austral summer 2012, i.e. from 20 January through 26 March, the classifier was operated with a so-called nano-DMA (nano differential mobility analyser, TSI Model 3085) in combination with a condensation particle counter (CPC, TSI model WCPC 3788, 50 % cut-off diameter $D_{p(50\%)}$ of 2.5 nm). We adjusted aerosol and sheath flow to achieve nominal aerosol size distribution measurements between 2.02 and 63.8 nm with a 64 channel resolution. Note that the SMPS primarily measured the electrical mobility of particles which was finally converted by a known transfer function to the corresponding particle mobility diameter D_p. Due to increased uncertainty caused by diffusional losses and cut-off corrections for the used CPC, we evaluated the data starting from 2.94 nm. All size spectra were multiple charge and diffusion corrected according to the TSI software AIM (Aerosol Instrument Manager®). The original spectra were taken with a scanning time of 120 s (retrace time 15 s) and the average size distribution of 4 consecutive spectra was stored for further evaluation, resulting in a temporal resolution of 600 s (duty cycle 480 s). During 2014 the measuring period was from 1 February through 30 April and from 12 August through 27 September. Due to technical problems we could not run the SMPS with the same configuration as in 2012, but used here a DMA model 3081 in combination with a CPC 3025A (TSI, $D_{p(50\%)}$ of 3 nm). Now, the air flow ratio was adjusted to enable size distribution measurements in the range be-

tween 6.26 and 212.9 nm. Note that due to the geometry of the DMA 3081, inherently longer particle residence time entailed perceptible particle losses resulting in enhanced uncertainties in the size distribution below 10 nm. Referred to Dal Maso et al. (2005), we will use the terms nucleation mode for particles with $D_p < 25$ nm and Aitken mode for the size range 25 nm $\leq D_p < 100$ nm throughout the text.

Particle size distributions were evaluated along with continuous long-term condensation particle (CP) concentration measurements (CPC 3022A, TSI, $D_{p(50\%)}$ of 7 nm) and the ionic composition of the aerosol. For the latter, bulk aerosol sampling was regularly conducted in 24 h time periods using a teflon and a nylon filter in series (all 1 μm pore size). According to Piel et al. (2006) and Weller and Lampert (2008) samples were analyzed by ion chromatography for methane sulfonate ($CH_3SO_3^-$, MS), Cl^-, Br^-, NO_3^-, SO_4^{2-}, Na^+, NH_4^+, K^+, Mg^{2+}, and Ca^{2+}.

Meteorological data were available from the Meteorological Observatory at NM (a description of the observatory itself and the installed meteorological sensors can be found under: http://www.awi.de/en/infrastructure/stations/neumayer_station/observatories/meteorological_observatory/, last access: 24 March 2015). The origin of the advected air masses was assessed by 5 days backward trajectories provided by HYSPLIT 4.0 (Hybrid Single-Particle Lagrangian Integrated trajectory; http://www.arl.noaa.gov/documents/reports/hysplit_user_guide.pdf, last access: 24 March 2015). For all trajectory calculations we used GDAS meteorological data with a spatial resolution of $1° \times 1°$ (longitude × latitude grid). HYSPLIT trajectories also provide a crude estimate of the vertical mixing height. In order to specify the characteristic of the local planetary boundary layer (PBL) we additionally gauged vertical mixing in that layer as described in Weller et al. (2011a, 2014) by using the local bulk Richardson number Ri_B (Stull, 1988).

2.2 Data evaluation methods

Particle concentrations, especially within the nucleation mode are susceptible to local contamination. Hence data recorded under potential contamination conditions, indicated by wind directions within a 330–30° sector and/or wind velocities below $2.0\,\mathrm{m\,s^{-1}}$ were removed. In addition black carbon (BC) concentrations were continuously monitored by a Multi Angle Absorption Photometer (MAAP model 5012, Thermo Electron Corp.), providing a supplemental criterion for local pollution when BC concentrations levels exceeded $100\,\mathrm{ng\,m^{-3}}$. Potential contamination happened only very sporadically within short periods (some hours at most) and on the whole, the actual data loss due to potential contamination was virtually negligible.

The crucial point of this study was to identify and characterize new particle formation. For this, we relied on the detailed criteria described by Dal Maso et al. (2005) and Kulmala et al. (2012). According to these recommendations, we defined a NPF event provided that particle size distribution starts within the nucleation mode ($D_p < 25\,\mathrm{nm}$) and prevailed for more than an hour. Due to the fact that we could not assume particle formation to occur generally across a wide area (some 100 km), but also by local natural sources (e.g. biogenic marine sulfur emissions from the nearby Atka Bay), we disregarded the particle growth criterion, which may then not be applicable (Dal Maso et al., 2005; O'Dowd et al., 2002a). If the recorded size distribution spectra indicated particle growth, the linear growth rate (GR), defined as the change in particle diameter ΔD_p (nm) during a time step Δt (h) was determined by the so-called mode fitting method and in addition by the method of maximum concentration (Dal Maso et al., 2005; Yli-Juuti et al., 2011; Kulmala et al., 2012). We assumed that the GR was constant throughout the event thus determined the GR by a linear fit through the geometric mean D_p (derived from the mode fitting procedure) at different times. In our case, nucleation mode and Aitken mode were generally well separated and log-normal distributions could be reliably fitted to the results. In contrast, the maximum concentration method resulted in somewhat higher GR compared to the mode fitting procedure (Table 1, values in

parenthesis). However, the latter approach was occasionally not successful thus we relied on the mode fitting method. Finally we estimated nucleation particle formation rate for the size range between 3 and 25 nm defined by:

$$J_{3-25} = \frac{\Delta N_{3-25}}{\Delta t} \tag{1}$$

Here, ΔN_{3-25} is the particle concentration in the size range between 3 and 25 nm derived from the SMPS data. Note that our approach to calculate particle formation as well as GR presumes a homogenous air mass and thus neglects the impact of changing air mass advection. Unfortunately, particle size distribution data were only available from 2.94 to 63.8 and 6.26 to 212.9 nm, respectively, hence an appropriate calculation of coagulation and condensation losses to correct GR and particle formation rate was impossible, but should usually be negligible in clean, homogeneous air masses (Kulmala et al., 2004a; Leppä et al., 2011). In fact, during both campaigns, total condensation particle (CP) concentrations measured by the CPC 3022A were typically below 1000 cm^{-3} and only very rarely reached 2000 cm^{-3}. In addition, during all NPF events nucleation mode particles ($D_p < 25$ nm) constituted the major component of the total CP concentration. According to Leppä et al. (2011), self-coagulation and coagulation scavenging might have distorted in our case growth rates well below 0.03 and 0.02 nm h^{-1}, respectively.

According to Nieminen et al. (2010) and Yli-Juuti et al. (2011), we finally estimated the H$_2$SO$_4$ vapour concentration needed for the calculated GR, assuming that H$_2$SO$_4$ was the sole component responsible for the observed particle growth:

$$GR = \frac{\gamma \cdot m_v \cdot v_{mol}}{2\rho} \cdot c_{vapour} \tag{2}$$

with m_v = molecular mass of the vapour (98 g mole^{-1}), ρ = density of the condensed vapour (1.6 g cm^{-3} assuming a H$_2$SO$_4$/H$_2$O mixture), v_{mol} = gas kinetic velocity of the

Natural new particle formation

R. Weller et al.

vapour molecules (e.g. $242\,\mathrm{m\,s^{-1}}$ for $T = 273\,\mathrm{K}$), c_{vapour} = gaseous H_2SO_4 concentration to be determined, and γ is close to the H_2SO_4 accommodation coefficient (assumed to be around 1.0).

3   Results

3.1   Data presentation

During the first summer campaign in 2012 (comprising 66 observation days and 9500 raw spectra) we identified 19 events of NPF without clearly discernible particle growth (class II events according to Dal Maso et al., 2005). Growth rates could be reliably determined in 8 class I or so-called "banana-type" events (Dal Maso et al., 2005). An overview of size resolved aerosol data for the months January through March 2012 as well as a selected series of consecutive NPF events is presented in the Supplement (Figs. S1 and S2) together with concurrently measured total CP concentrations, meteorological parameters, and the ionic composition of the bulk aerosol (data from both campaigns reported here are available at doi:10.1594/PANGAEA.845024). Figure 1 on the other hand focuses on a striking NPF event happened in 27 January, where a simultaneous nucleation- and Aitken mode growth was evident. Figure 2 shows a more detailed topographic view of this event on a linear $\mathrm{d}N/\mathrm{d}\log D_{\mathrm{p}}$ scale and is supplemented by corresponding profiles of log-normal distribution fits from selected time slices. In addition, a strikingly prolonged Aitken mode growth over about 3 days ($\mathrm{GR} = 0.3 \pm 0.05\,\mathrm{nm\,h^{-1}}$) started at 1 March (doy 61) but without exhibiting a discernible nucleation mode (Fig. S2). Particle concentrations in the nucleation mode were strongly correlated with total CP concentrations measured by the CPC 3022A (Fig. S1b). A correlation of particle concentrations measured by the SMPS in the range between 5 and 64 nm with CP concentrations revealed a linear dependence (slope 0.992, $r^2 = 0.8$; see Fig. S3 in the Supplement), indicating that during summer CP number concentrations were dominated by nucleation and Aitken mode particles.

In contrast, the yield of NPF events during summer 2014 (February through April 2014, 85 observation days, 12 240 raw spectra) was rather scanty: apart from 15 class II events, only 2 class I events could be discerned. A presentation of this time series can again be found in the Supplement (Fig. S4). During winter (August and September 2014, 37.5 observation days, 5370 raw spectra), two certain class II events were evident (14/15 August and 21 September, Fig. 3). Figure 4 presents the mean particle size distribution during both winter events and for comparison for a typical non-event day (18 August 2014). Table 1 summarizes all evaluated class I events and lists the calculated GR, nucleation particle formation rates (J_{3-25}) and the estimated H_2SO_4 concentration hypothetically needed for the respective GR.

3.2 Meteorological aspects

Regarding local meteorology, virtually all NPF events observed at NM occurred during southerly wind directions ($180 \pm 60°$) with wind velocities below $12\,\mathrm{m\,s^{-1}}$ (typically between 4 and $8\,\mathrm{m\,s^{-1}}$) and mostly bright weather conditions prevailed. In all cases the local PBL was characterized by Ri_B numbers < 0.25, indicating turbulent flow and a well-mixed PBL. This was supported by HYSPLIT back trajectory analyses indicating vertical mixing heights around 250 m (range: 100 to 600 m) for the last 6 h before arrival at NM (5 days back trajectories for the most prominent nucleation events are presented in the Supplement, Fig. S5). Note, however that mixing heights provided by HYSPLIT should be treated as a rough estimate, particularly regarding the Antarctica PBL due to the impact of katabatic winds and the fact that vertical wind components could be somewhat uncertain for regions with sparse meteorological input data. The spatial extend of NPF events associated with appreciable particle growth could be estimated to be around 170 ± 85 km, taking into account the prevailing wind velocity (around $8 \pm 4\,\mathrm{m\,s^{-1}}$) and the confined NPF duration (around 6 h, Table 1). Corresponding backward trajectories revealed that air masses typically travelled along the Antarctic coastline up to five days before arrival at NM (Fig. S5). The contact time of these trajectories with open water or sea ice appeared rather limited and often happened just

some hours before arrival at NM. In general, during NPF events trajectories stayed below 1000 m above ground for the last 48 h before arrival at NM and mainly within the vertical mixing heights derived from HYSPLIT for the last 24 h. Only for the NPF event at 16 March 2012 air masses clearly descended from the free troposphere (in this case > 2000 m above ground) within the last 24 h before arrival at NM.

During summer, nucleation events showed a distinct diurnal cycle. They typically occurred in the second half of the day indicating a link to local photochemistry, though being sometimes delayed to the diurnal maximum of UV radiation by a few hours (Figs. 1 and S2; Table 1). In contrast, winter events happened either several hours around midnight or more than day-long (Fig. 3). Again, respecting 5 days back trajectories documented a similar advection pattern as for the summertime NPF events (Fig. S6).

During stormy weather, occasionally enhanced particle concentrations appeared below 10 nm. In this context, it is worth to mention that Virkkula et al. (2007) and Asmi et al. (2010) observed at Aboa some nucleation events associated with high wind speeds and suggested ion production by fast moving ice crystals followed by subsequent ion-mediated nucleation. As for NM the situation was somewhat unclear, because charged particle concentration data were not available and during stormy weather the overall electrostatic charge in combination with inherently critical electrical grounding conditions on ice may have provoked instrumental artefacts.

4 Discussion

4.1 Extent of particle growth

In view of previous results from Antarctica (Asmi et al., 2010; Järvinen et al., 2013; Kyrö et al., 2013), NPF at NM appeared notably less efficient. Particle growth was usually confined to the nucleation mode and only once extended into the Aitken mode (at 27 January 2012, Table 1 and Figs. 1 and 2). Regarding the latter observation, a first

NPF event started at 07:00 UTC with a mode mean particle size of 18.7 nm finally reaching 33.7 nm at 14:00 UTC (Table 1 and Figs. 1a and 2). Simultaneously a second NPF started at 11:00 UTC, while the total particle number concentrations instantly increased up to 3000 cm^{-3}. Figure 1b indicated that concentrations of particles with $D_p > 25$ nm were between 1000 and 1500 cm^{-3} finally reaching a mode mean diameter around 50 nm in late 29 January (Fig. 1a). Consequently, this NPF event was the only one at NM where the growth of nucleated particles extended into a size range potentially relevant for acting as CCN. On the other hand, a persistent, but not locally developed Aitken mode was often present during polar day (Fig. S1) and after being missing in August reappeared in September (Fig. 3). Notwithstanding some discrete events with strikingly high particle concentrations between 30 and 200 nm occurred in August exclusively under stormy weather (wind velocity around 20 m s^{-1}; Fig. 3). According to impactor measurents conducted by Teinilä et al. (2014) in the year 2010 at NM, most probably sub-µm sea salt aerosol might also have caused the latter peculiarities.

4.2 Role of DMS derived sulfuric acid and MSA

In conjunction with the observed diurnal cycle and air mass advection pattern, particle nucleation at NM was most probably induced by nearby emissions of marine biogenic precursor gases (Yu and Luo, 2010). More precisely, photo-oxidation of phytoplankton derived dimethyl sulfide (DMS) is in general the prominent photochemical process in the troposphere of coastal Antarctica (e.g. Minikin et al., 1998), yielding ultimately sulfuric acid (H$_2$SO$_4$) and methane sulfonic acid (MSA, CH$_3$SO$_3$H). Nevertheless, and in agreement with results from other Antarctic sites (Järvinen et al., 2013; Kyrö et al., 2013), H$_2$SO$_4$ concentrations needed for the observed growth rates should be at least an order of magnitude higher compared to available values actually observed in Antarctica: Jefferson et al. (1998) measured mean H$_2$SO$_4$ concentrations around 1.6×10^6 molec cm^{-3} during the SCATE campaign at Palmer Station (Antarctic Peninsula) in summer, and at South Pole during the ISCAT 2000 campaign H$_2$SO$_4$ (MSA)

concentrations around 0.27×10^6 molec cm^{-3} (0.08×10^6 molec cm^{-3}) were detected in December (Mauldin III et al., 2004). Although the chemical composition of secondary aerosol during summer at NM was usually dominated by DMS derived nss-SO$_4^{2-}$ and MS (Weller and Lampert, 2008; Weller et al., 2011b), observed particle growth should yet be controlled by other low volatile vapours.

4.3 Possible role of H$_2$O vapour, NH$_3$, organic vapour, and iodine oxide

Theoretical and laboratory studies revealed that H$_2$O molecules are important for early particle growth (2–3 nm) due to stabilization of the critical nucleus by H$_2$SO$_4$-hydrate formation, while further particle growth is dominated by H$_2$SO$_4$ or low volatile organic vapours (Nieminen et al., 2010; Zhang et al., 2012). These investigations indicated that under prevalent atmospheric conditions nucleation rate might be correlated with relative humidity (RH), depending on NH$_3$ and organic vapour concentrations (Zhang et al., 2012). Concerning this point, our data were inconclusive: it seems, though in contrast to the above mentioned investigations, that NPF events sometimes occurred during RH decrease (Fig. S2). But this apparent correlation was particularly due to the fact that we mainly observed NPF in the afternoon when increasing temperatures usually induced decreasing RH levels. In addition, a correlation between H$_2$O vapour partial pressure and nucleation rates derived from Eq. (1) was absent.

Apart from H$_2$SO$_4$ and H$_2$O vapour, gaseous precursors like NH$_3$, organic vapours (notably organic amines), and inorganic iodine compounds (mainly iodine oxides) are known to be strongly involved in particle nucleation and particle growth (O'Dowd et al., 2002b; Kulmala et al., 2004b; Facchini et al., 2008a; McFiggans et al., 2010; Metzger et al., 2010; Benson et al., 2011; Dawson et al., 2012; Riccobono et al., 2012; Riipinen et al., 2012; Wang et al., 2013). As for NH$_3$, previous thermodenuder measurements at NM indicated that biogenic secondary aerosol was likely an internal mixture of the acids H$_2$SO$_4$ and MSA partly neutralized by NH$_3$ (Weller et al., 2011a). Actually, we observed NH$_4^+$ concentrations at NM of around 10 ng m^{-3}. Preliminary results on the amount

of water soluble organic carbon (WSOC, excluding MSA), determined from bulk filter samples taken during austral summer 2011 showed values between 5 and 35 ngC m^{-3} (method: solid phase extraction followed by TOC analysis; J. Lehmann, personal communication, 2015). Interestingly, NH$_4^+$ and WSOC concentrations appeared thus similar to values reported from Aboa (Asmi et al., 2010) where particle growth was more pronounced. At Aboa, biogenic emissions by nearby melting ponds were found to be a potential source for condensable vapour (Kyrö et al., 2013), while the surroundings of NM are completely ice covered throughout (apart from open water dependent on seasonal sea ice coverage) and the nearest insular rocky outcrops are more than 200 km away. One may speculate that marine primary organic aerosol was dominant at NM, linked with sea spray formation by bubble bursting (Facchini et al., 2008b), while at Aboa condensable organic vapour emissions from melting ponds were decisive.

Concerning iodine compounds, in situ measurements by long-path Differential Optical Absorption Spectroscopy (DOAS) conducted at Halley (Saiz-Lopez et al., 2007) as well as respective satellite observations (Schönhardt et al., 2012) revealed maximum IO concentration of some 5 pptv (volume parts per trillion) over Antarctic coastal regions around October. Such IO levels were comparable to coastal European sites like Roscoff and Mace Head (O'Dowd et al., 2002b; McFiggans et al., 2010). At NM, previous DOAS measurements using scattered sunlight primarily provided IO column densities, but presuming that IO was restricted within the PBL (below 2 km), comparable IO mixing ratios in the range of some pptv were detected (Frieß et al., 2001, 2010). Interestingly, at Dumont d'Urville (DDU), IO concentrations were found to be an order of magnitude lower indicating that halogen chemistry in general was probably promoted by the much larger sea ice extend of the Atlantic sector of Antarctica (Grilli et al., 2013). From the mid-latitude European sites Roscoff and Mace Head there exists strong evidence for iodine mediated NPF (O'Dowd et al., 2002b; McFiggans et al., 2010) and in a recent study, a possible impact of IO on NPF in the Arctic was inferred (Allan et al., 2015). In view of the minor importance of DMS photochemistry, we speculate that IO probably initiated the observed NPF at NM in late winter. The shape of both winter

events and the fact that growth rates could not be determined indicated a local origin where particle size distribution developed during transport time to the measuring site (Kulmala et al., 2012).

5 Conclusions

In summary, NPF events were most likely mediated by $H_2SO_4/NH_3/H_2O$ ternary nucleation during summer at NM, while the observed particle growth was governed by the availability of other yet not identified gaseous precursors, most probably low volatile organic compounds of marine origin. Due to the apparent deficit of the latter, particle growth was accordingly restricted within the nucleation mode and in the main did not extend to particle diameter ranges relevant for acting as cloud condensation nuclei. Given that particle growth in the early stage (i.e. within the nucleation mode) was governed by low volatile vapours other than H_2SO_4, another remaining crucial question is, in which way the finally sulfuric acid dominated secondary aerosol at NM was ultimately generated. During summer, a potential role of iodine oxides in particle nucleation was unclear, while for the observed winter events these compounds could be potential candidates. But then, the even more pronounced deficit of condensable vapour due to depressed photochemical activity impeded particle growth beyond particle diameters of about 15 nm.

In conclusion, our investigations indicate three crucial points concerning NPF in Antarctica that are supposed to be addressed in future work: (i) up to now, from this region only sparse and inadequate knowledge exists on organic aerosols, in particular secondary organic aerosol. Identification of the most important compounds, their origin and source strength is still fragmentary at best. (ii) IO concentrations should be measured year-round by in-situ techniques in order to better assess its role in NPF and validate respecting satellite retrievals. (iii) The role of free tropospheric air in providing gaseous precursor for particle nucleation and growth within the PBL needs clarifica-

tion. This point appeared especially important for continental Antarctica in view of the recently described NPF events observed at Dome C (Järvinen et al., 2013).

The Supplement related to this article is available online at doi:10.5194/acpd-15-15655-2015-supplement.

References

Allan, J. D., Williams, P. I., Najera, J., Whitehead, J. D., Flynn, M. J., Taylor, J. W., Liu, D., Darbyshire, E., Carpenter, L. J., Chance, R., Andrews, S. J., Hackenberg, S. C., and McFiggans, G.: Iodine observed in new particle formation events in the Arctic atmosphere during ACCACIA, Atmos. Chem. Phys., 15, 5599–5609, doi:10.5194/acp-15-5599-2015, 2015.

Asmi, E., Frey, A., Virkkula, A., Ehn, M., Manninen, H. E., Timonen, H., Tolonen-Kivimäki, O., Aurela, M., Hillamo, R., and Kulmala, M.: Hygroscopicity and chemical composition of Antarctic sub-micrometre aerosol particles and observations of new particle formation, Atmos. Chem. Phys., 10, 4253–4271, doi:10.5194/acp-10-4253-2010, 2010.

Benson, D. R., Yu, J. H., Markovich, A., and Lee, S.-H.: Ternary homogeneous nucleation of H_2SO_4, NH_3, and H_2O under conditions relevant to the lower troposphere, Atmos. Chem. Phys., 11, 4755–4766, doi:10.5194/acp-11-4755-2011, 2011.

Boucher, O., Randall, D., Artaxo, P., Bretherton, C., Feingold, G., Forster, P., Kerminen, V.-M., Kondo, Y., Liao, H., Lohmann, U., Rasch, P., Satheesh, S. K., Sherwood, S., Stevens, B., and

Natural new particle formation

R. Weller et al.

⏮ | ⏭

◀ | ▶

Back | Close

Full Screen / Esc

Printer-friendly Version

Interactive Discussion

Zhang, X. Y.: Clouds and aerosols, in: Climate Change 2013: the Physical Science Basis. Contribution of Working Group I to the Fifth Assessment Report of the Intergovernmental Panel on Climate Change, edited by: Stocker, T. F., Qin, D., Plattner, G.-K., Tignor, M., Allen, S. K., Boschung, J., Nauels, A., Xia, Y., Bex, V., and Midgley, P. M., 614–623, Cambridge University Press, Cambridge, UK, New York, NY, USA, 2013.

Bzdek, B. and Johnston, M. V.: New particle formation and growth in the troposphere, Anal. Chem., 82, 7871–7878, doi:10.1021/ac100856j, 2010.

Carslaw, K. S., Lee, L. A., Reddington, C. L., Pringle, K. J., Rap, A., Forster, P. M., Mann, G. W., Spracklen, D. V., Woodhouse, M. T., Regayre, L. A., and Pierce, J. R.: Large contribution of natural aerosol to uncertainty in indirect forcing, Nature, 503, 67–71, doi:10.1038/nature12674, 2013.

Dal Maso, M., Kulmala, M., Riipinen, I., Wagner, R., Hussein, T., Aalto, P. P., and Lehtinen, E. J.: Formation and growth of fresh atmospheric aerosols: eight years of aerosol size distribution data from SMEAR II, Hyytiälä, Finland, Boreal Environ. Res., 10, 323–336, 2005.

Dawson, M. L., Varner, M. E., Perraud, V., Ezell, M. J., Gerber, R. B., and Finlayson-Pitts, B. J.: Simplified mechanism for new particle formation from methanesulfonic acid, amines, and water via experiments and ab initio calculations, P. Natl. Acad. Sci. USA, 109, 18719–18724, doi:10.1073/pnas.1211878109, 2012.

Facchini, M. C., Decesari, S., Rinaldi, M., Carbone, C., Finessi, E., Mircea, M., Fuzzi, S., Moretti, F., Tagliavini, E., Ceburnis, D., and O'Dowd, C. D.: Important source of marine secondary organic aerosol from biogenic amines, Environ. Sci. Technol., 42, 9116–9121, 2008a.

Facchini, M. C., Rinaldi, M., Decesari, S., Carbone, C., Finessi, E., Mircea, M., Fuzzi, S., Ceburnis, D., Flanagan, R., Nilsson, E. D., de Leeuw, G., Martino, M., Woeltjen, J., and O'Dowd, C. D.: Primary submicron marine aerosol dominated by insoluble organic colloids and aggregates, Geophys. Res. Lett., 35, L17814, doi:10.1029/2008GL034210, 2008b.

Frieß, U., Wagner, T., Pundt, I., Pfeilsticker, K., and Platt, U.: Spectroscopic measurements of troposheric iodine oxide at Neumayer Station, Antarctica, Geophys. Res. Lett., 28, 1941–1944, doi:10.1029/2000GL012784, 2001.

Frieß, U., Deutschmann, T., Gilfedder, B. S., Weller, R., and Platt, U.: Iodine monoxide in the Antarctic snowpack, Atmos. Chem. Phys., 10, 2439–2456, doi:10.5194/acp-10-2439-2010, 2010.

Grilli, R., Legrand, M., Kukui, A., Méjean, G., Preunkert, S., and Romanini, D.: First investigations of IO, BrO, and NO_2 summer atmospheric levels at a coastal East Antarctic site using

mode-locked cavity enhanced absorption spectroscopy, Geophys. Res. Lett., 40, 791–796, doi:10.1002/grl.50154, 2013.

Haywood, J. and Boucher, O.: Estimates of the direct and indirect radiative forcing due to tropospheric aerosols: a review, Rev. Geophys., 38, 513–543, 2000.

Henze, D. K. and Seinfeld, J. H.: Global secondary organic aerosol from isoprene oxidation, Geophys. Res. Lett., 33, L09812, doi:10.1029/2006GL025976, 2006.

Ito, T.: Study of background aerosols in the Antarctic troposphere, J. Atmos. Chem., 3, 69–91, 1985.

Ito, T.: Size distribution of Antarctic submicron aerosols, Tellus B, 45, 145–159, 1993.

Jaenicke, R., Dreiling, V., Lehmann, E., Koutsenoguii, P. K., and Stingl, J.: Condensation nuclei at the German Antarctic Station "Georg von Neumayer", Tellus B, 44, 311–317, 1992.

Järvinen, E., Virkkula, A., Nieminen, T., Aalto, P. P., Asmi, E., Lanconelli, C., Busetto, M., Lupi, A., Schioppo, R., Vitale, V., Mazzola, M., Petäjä, T., Kerminen, V.-M., and Kulmala, M.: Seasonal cycle and modal structure of particle number size distribution at Dome C, Antarctica, Atmos. Chem. Phys., 13, 7473–7487, doi:10.5194/acp-13-7473-2013, 2013.

Jefferson, A., Tanner, D. J., Eisele, F. L., Davis, D. D., Chen, G., Crawford, J., Huey, J. W., Torres, A. L., and Berresheim, H.: OH photochemistry and methane sulfonic acid formation in the coastal Antarctic boundary layer, J. Geophys. Res., 103, 1647–1656, 1998.

König-Langlo, G., King, J. C., and Pettré, P.: Climatology of the three coastal Antarctic stations Dumont d'Urville, Neumayer and Halley, J. Geophys. Res., 103, 10935–10946, 1998.

Koponen, I. K., Virkkula, A., Hillamo, R., Kerminen, V.-M., and Kulmala, M.: Number size distribution and concentrations of the continental summer aerosol in Queen Maud Land, Antarctica, J. Geophys. Res., 108, 4587, doi:10.1029/2003JD003614, 2003.

Korhonen, H., Carslaw, K. S., Spracklen, D. V., Mann, G. W., and Woodhouse, M. T.: Influence of oceanic dimethyl sulfide emissions on cloud condensation nuclei concentrations and seasonality over the remote Southern Hemisphere oceans: a global model study, J. Geophys. Res., 113, D15204, doi:10.1029/2007JD009718, 2008.

Kulmala, M., Vehkamäki, H., Petäjä, T., Dal Maso, M., Lauri, A., Kerminen, V.-M., Birmili, W., and McMurry, P. H.: Formation and growth rates of ultrafine atmospheric particles: a review of observations, J. Aerosol Sci., 35, 143–176, doi:10.1016/j.jaerosci.2003.10.003, 2004a.

Kulmala, M., Kerminen, V.-M., Anttila, T., Laaksonen, A., and O'Dowd, D.: Organic aerosol formation via sulphate cluster activation, J. Geophys. Res., 109, D04205, doi:10.1029/2003JD003961, 2004b.

Natural new particle formation

R. Weller et al.

Kulmala, M., Petäjä, T., Nieminen, T., Sipilä, M., Manninen, H. E., Lehtipalo, K., Dal Maso, M., Aalto, P. P., Junninen, H., Paasonen, P., Riipinen, I., Lehtinen, K. E. J., Laaksonen, A., and Kerminen, V.-M.: Measurements of the nucleation of atmospheric aerosol particles, Nat. Protoc., 7, 1651–1667, doi:10.1038/nprot.2012.091, 2012.

Kyrö, E.-M., Kerminen, V.-M., Virkkula, A., Dal Maso, M., Parshintsev, J., Ruíz-Jimenez, J., Forsström, L., Manninen, H. E., Riekkola, M.-L., Heinonen, P., and Kulmala, M.: Antarctic new particle formation from continental biogenic precursors, Atmos. Chem. Phys., 13, 3527–3546, doi:10.5194/acp-13-3527-2013, 2013.

Leppä, J., Anttila, T., Kerminen, V.-M., Kulmala, M., and Lehtinen, K. E. J.: Atmospheric new particle formation: real and apparent growth of neutral and charged particles, Atmos. Chem. Phys., 11, 4939–4955, doi:10.5194/acp-11-4939-2011, 2011.

Mauldin III, R. L., Kosciuch, E., Henry, B., Eisele, F. L., Shetter, R., Lefer, B., Chen, G., Davis, D., Huey, G., and Tanner, D.: Measurements of OH, $HO_2 + RO_2$, H_2SO_4, and MSA at the South Pole during ISCAT 2000, Atmos. Environ., 38, 5423–5437, 2004.

McFiggans, G., Bale, C. S. E., Ball, S. M., Beames, J. M., Bloss, W. J., Carpenter, L. J., Dorsey, J., Dunk, R., Flynn, M. J., Furneaux, K. L., Gallagher, M. W., Heard, D. E., Hollingsworth, A. M., Hornsby, K., Ingham, T., Jones, C. E., Jones, R. L., Kramer, L. J., Langridge, J. M., Leblanc, C., LeCrane, J.-P., Lee, J. D., Leigh, R. J., Longley, I., Mahajan, A. S., Monks, P. S., Oetjen, H., Orr-Ewing, A. J., Plane, J. M. C., Potin, P., Shillings, A. J. L., Thomas, F., von Glasow, R., Wada, R., Whalley, L. K., and Whitehead, J. D.: Iodine-mediated coastal particle formation: an overview of the Reactive Halogens in the Marine Boundary Layer (RHaMBLe) Roscoff coastal study, Atmos. Chem. Phys., 10, 2975–2999, doi:10.5194/acp-10-2975-2010, 2010.

Metzger, A., Verheggen, B., Dommen, J., Duplissy, J., Prevot, A. S. H., Weingartner, E., Riipinen, I., Kulmala, M., Spracklen, D. V., Carslaw, K. S., and Baltensperger, U.: Evidence for the role of organics in aerosol particle formation under atmospheric conditions, P. Natl. Acad. Sci. USA, 107, 6646–6651, doi:10.1073/pnas.0911330107, 2010.

Minikin, A., Legrand, M., Hall, J., Wagenbach, D., Kleefeld, C., Wolff, E., Pasteur, E. C., and Ducroz, F.: Sulfur-containing species (sulfate and methanesulfonate) in coastal Antarctic aerosol and precipitation, J. Geophys. Res., 103, 10975–10990, 1998.

Nieminen, T., Lehtinen, K. E. J., and Kulmala, M.: Sub-10 nm particle growth by vapor condensation – effects of vapor molecule size and particle thermal speed, Atmos. Chem. Phys., 10, 9773–9779, doi:10.5194/acp-10-9773-2010, 2010.

Title Page

Abstract | Introduction

Conclusions | References

Tables | Figures

|◀ | ▶|

◀ | ▶

Back | Close

Full Screen / Esc

Printer-friendly Version

Interactive Discussion

O'Dowd, C. D. and de Leeuw, G.: Marine aerosol production: a review of the current knowledge, Philos. T. Roy. Soc. A, 365, 1753–1774, doi:10.1098/rsta.2007.2043, 2007.

O'Dowd, C. D., Hämeri, K., Mäkelä, J. M., Pirjola, L., Kulmala, M., Jennings, S. G., Berresheim, H., Hansson, H.-C., de Leeuw, G., Kunz, G. J., Allen, A. G., Hewitt, C. N., Jackson, A., Viisanen, Y., and Hoffmann, T.: A dedicated study of New Particle Formation and Fate in the Coastal Environment (PARFORCE): overview of objectives and achievements, J. Geophys. Res., 107, 8108, doi:10.1029/2001JD000555, 2002a.

O'Dowd, C. D., Jimenez, J. L., Bahreini, R., Flagan, R. C., Seinfeld, J. H., Hämeri, K., Pirjola, L., Kulmala, M., Jennings, S. G., and Hoffmann, T.: Marine aerosol formation from biogenic iodine emissions, Nature, 417, 632–636, doi:10.1038/nature00775, 2002b.

Park, J., Sakurai, H., Vollmers, K., McMurry, P. H.: Aerosol size distributions measured at South Pole during ISCAT, Atmos. Environ., 38, 5493–5500, doi:10.1016/j.atmosenv.2002.12.001, 2004.

Piel, C., Weller, R., Huke, M., and Wagenbach, D.: Atmospheric methane sulfonate and non-sea salt sulphate records at the EPICA deep-drilling site in Dronning Maud Land, Antarctica, J. Geophys. Res., 111, D03304, doi:10.1029/2005JD006213, 2006.

Ramanathan, V., Crutzen, P. J., Kiehl, J. T., and Rosenfeld, D.: Aerosols, climate, and the hydrological cycle, Science, 294, 2119–2124, 2001.

Riccobono, F., Rondo, L., Sipilä, M., Barmet, P., Curtius, J., Dommen, J., Ehn, M., Ehrhart, S., Kulmala, M., Kürten, A., Mikkilä, J., Paasonen, P., Petäjä, T., Weingartner, E., and Baltensperger, U.: Contribution of sulfuric acid and oxidized organic compounds to particle formation and growth, Atmos. Chem. Phys., 12, 9427–9439, doi:10.5194/acp-12-9427-2012, 2012.

Riipinen, I., Yli-Juuti, T., Pierce, J. R., Petäjä, T., Worsnop, D. R., Kulmala, M., and Donahue, N. M.: The contribution of organics to atmospheric nanoparticle growth, Nat. Geosci., 5, 453–458, doi:10.1038/ngeo1499, 2012.

Rosenfeld, D., Andreae, M. O., Asmi, A., Chin, M., de Leeuw, G., Donovan, D. P., Kahn, R., Kinne, S., Kivekäs, N., Kulmala, M., Lau, W., Schmidt, K. S., Suni, T., Wagner, T., Wild, M., and Quaas, J.: Global observations of aerosol–cloud-precipitation–climate interactions, Rev. Geophys., 52, 750–808, doi:10.1002/2013RG000441, 2014.

Saiz-Lopez, A., Mahajan, A. S., Salmon, R. A., Bauguitte, J.-B., Jones, A. E., Roscoe, H. K., and Plane, J. M. C.: Boundary Layer Halogens in Coastal Antarctica, Science, 317, 348–351, doi:10.1126/science.1141408, 2007.

Natural new particle formation

R. Weller et al.

Schönhardt, A., Begoin, M., Richter, A., Wittrock, F., Kaleschke, L., Gómez Martín, J. C., and Burrows, J. P.: Simultaneous satellite observations of IO and BrO over Antarctica, Atmos. Chem. Phys., 12, 6565–6580, doi:10.5194/acp-12-6565-2012, 2012.

Spracklen, D. V., Carslaw, K. S., Kulmala, M., Kerminen, V.-M., Mann, G. W., and Sihto, S.-L.: The contribution of boundary layer nucleation events to total particle concentrations on regional and global scales, Atmos. Chem. Phys., 6, 5631–5648, doi:10.5194/acp-6-5631-2006, 2006.

Spracklen, D. V., Carslaw, K. S., Kulmala, M., Kerminen, V.-M., Sihto, S.-L., Riipinen, I., Merikanto, J., Mann, G. W., Chipperfield, M. P., Wiedensohler, A., Birmili, W., and Lihavainen, H.: Contribution of particle formation to global cloud condensation nuclei concentrations, Geophys. Res. Lett., 35, L06808, doi:10.1029/2007GL033038, 2008.

Stull, R. B.: An Introduction to Boundary Layer Meteorology, Kluwer Academic Publishers, Dordrecht, 175–180, 1988.

Teinilä, K., Frey, A., Hillamo, R., Tülp, H. C., and Weller, R.: A study of the sea-salt chemistry using size-segregated aerosol measurements at coastal Antarctic station Neumayer, Atmos. Environ., 96, 11–19, 2014.

Virkkula, A., Hirsikko, A., Vana, M., Aalto, P. P., Hillamo, R., and Kulmala, M.: Charged particle size distributions and analysis of particle formation events at the Finnish Antarctic research station Abao, Boreal Environ. Res., 12, 397–408, 2007.

Wang, S. C. and Flagan, R. C.: Scanning electrical mobility spectrometer, Aerosol Sci. Tech., 13, 230–240, 1990.

Wang, J., McGraw, R. L., and Kuang, C.: Growth of atmospheric nano-particles by heterogeneous nucleation of organic vapor, Atmos. Chem. Phys., 13, 6523–6531, doi:10.5194/acp-13-6523-2013, 2013.

Weller, R. and Lampert, A.: Optical properties and sulfate scattering efficiency of boundary layer aerosol at coastal Neumayer Station, Antarctica, J. Geophys. Res., 113, D16208, doi:10.1029/2008JD009962, 2008.

Weller, R., Minikin, A., Wagenbach, D., and Dreiling, V.: Characterization of the inter-annual, seasonal, and diurnal variations of condensation particle concentrations at Neumayer, Antarctica, Atmos. Chem. Phys., 11, 13243–13257, doi:10.5194/acp-11-13243-2011, 2011a.

Weller, R., Wagenbach, D., Legrand, M., Elsässer, C., Tian-Kunze, X., and König-Langlo, G.: Continuous 25-years aerosol records at coastal Antarctica – 1: inter-annual variability of

ionic compounds and links to climate indices, Tellus B, 63, 901–919, doi:10.1111/j.1600-0889.2011.00542.x, 2011b.

Weller, R., Levin, I., Schmithüsen, D., Nachbar, M., Asseng, J., and Wagenbach, D.: On the variability of atmospheric ^{222}Rn activity concentrations measured at Neumayer, coastal Antarctica, Atmos. Chem. Phys., 14, 3843–3853, doi:10.5194/acp-14-3843-2014, 2014.

Yli-Juuti, T., Nieminen, T., Hirsikko, A., Aalto, P. P., Asmi, E., Hõrrak, U., Manninen, H. E., Patokoski, J., Dal Maso, M., Petäjä, T., Rinne, J., Kulmala, M., and Riipinen, I.: Growth rates of nucleation mode particles in Hyytiälä during 2003–2009: variation with particle size, season, data analysis method and ambient conditions, Atmos. Chem. Phys., 11, 12865–12886, doi:10.5194/acp-11-12865-2011, 2011.

Yu, F. and Luo, G.: Oceanic dimethyl sulfide emission and new particle formation around the coast of Antarctica: a modeling study of seasonal variations and comparison with measurements, Atmosphere, 1, 34–50, doi:10.3390/atmos1010034, 2010.

Zhang, R., Khalizov, A., Wang, L., Hu, M., and Xu, W.: Nucleation and growth of nanoparticles in the atmosphere, Chem. Rev., 112, 1957–2011, doi:10.1021/cr2001756, 2012.

Table 1. Nucleation events of class I (Dal Maso et al., 2005) during austral summer 2012 and 2014: time period during which the particle growth in the given range was observed, growth rate determined by log normal mode fitting and maximum concentration (in parenthesis) method, particle formation rate in the size range 3 to 25 nm ($J_{3–25}$), and estimated H_2SO_4 vapour concentration needed for the observed growth rate.

Date (doy 2012)	Time period	Growth rate ($nm\,h^{-1}$)	Range (nm)	$J_{3–25}$ (s^{-1})	H_2SO_4 needed ($molec\,cm^{-3}$)
27 Jan 2012 (27)	07:00–14:00	1.9 ± 0.1 (2.5 ± 0.3)	18.7–33.7	0.1 ± 0.05	7.3×10^7
	11:00–18:00	1.8 ± 0.1 (2.1 ± 0.3)	6.8–20.2	n.d.[a]	6.6×10^7
23 Feb 2012 (54)	12:00–18:00	0.61 ± 0.07 (n.d.)	4.9–8.9	0.1 ± 0.03	2.4×10^7
25 Feb 2012 (56)	13:00–17:00	0.87 ± 0.07 (n.d.)	5.2–8.4	0.03 ± 0.01	3.3×10^7
27 Feb 2012 (58)	11:00–18:00	1.0 ± 0.05 (1.1 ± 0.15)	11.6–18.5	0.06 ± 0.02	3.7×10^7
	13:00–18:00	0.87 ± 0.09 (1.0 ± 0.2)	5.2–9.1	0.06 ± 0.02	3.7×10^7
8 Mar 2012 (68)	08:00–17:00	0.83 ± 0.04 (1.0 ± 0.1)	7.8–14.8	0.02 ± 0.01	3.2×10^7
9 Mar 2012 (69)	14:00–19:00	0.84 ± 0.08 (1.4 ± 0.3)	5.2–9.1	0.08 ± 0.03	3.7×10^7
16 Mar 2012 (76)	10:00–16:00	0.8 ± 0.1 (1.5 ± 0.6)	13.2–18.3	0.07 ± 0.02	3.0×10^7
	14:00–21:00	1.0 ± 0.09 (1.1 ± 0.2)	5.9–12.9	0.09 ± 0.03	1.8×10^7
24 Mar 2012 (84)	15:00–19:00	0.5 ± 0.05 (n.d.)	4.1–6.1	0.02 ± 0.01	2.7×10^7
6 Feb 2014	14:00–19:00	0.4 ± 0.2[b] (n.d.)	8.8–11.3[b]	n.d.[c]	1.5×10^7
24 Mar 2014	11:00–18:00	0.46 ± 0.1 (n.d.)	14.5–16.6	n.d.[c]	1.7×10^7

[a] n.d. = not determined.
[b] Measured with the long DMA (TSI model 3081) with enhanced uncertainty below 10 nm.
[c] Particle formation rate not determined due to higher cut-off of the SMPS used during this period.

Full Screen / Esc
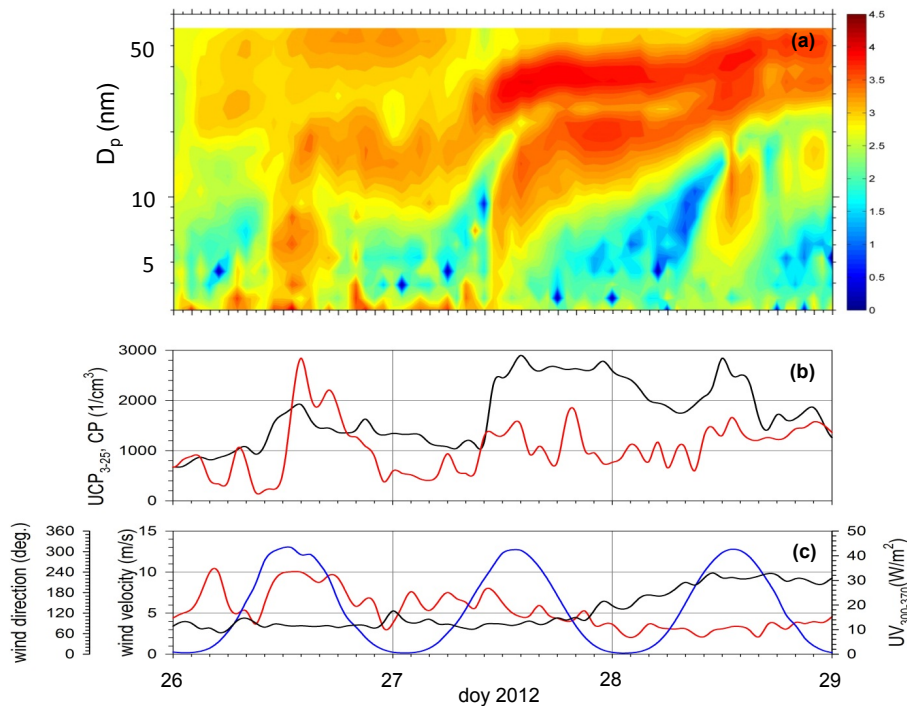
Figure 1. Time series of the measured particle size distribution $dN/d\log D_p$ (cm^{-3}) on a logarithmic scale (color code to the right of the contour plot) of a NPF event around 27 January 2012 showing a growing nucleation and Aitken mode **(a)**, corresponding CP concentration (black line) and particle concentrations between 3 and 25 nm (UCP$_{3-25}$, red line) **(b)**, wind velocity (red line) and wind direction (black line) and UV radiation at wavelengths between 300 and 370 nm (blue line) **(c)**.
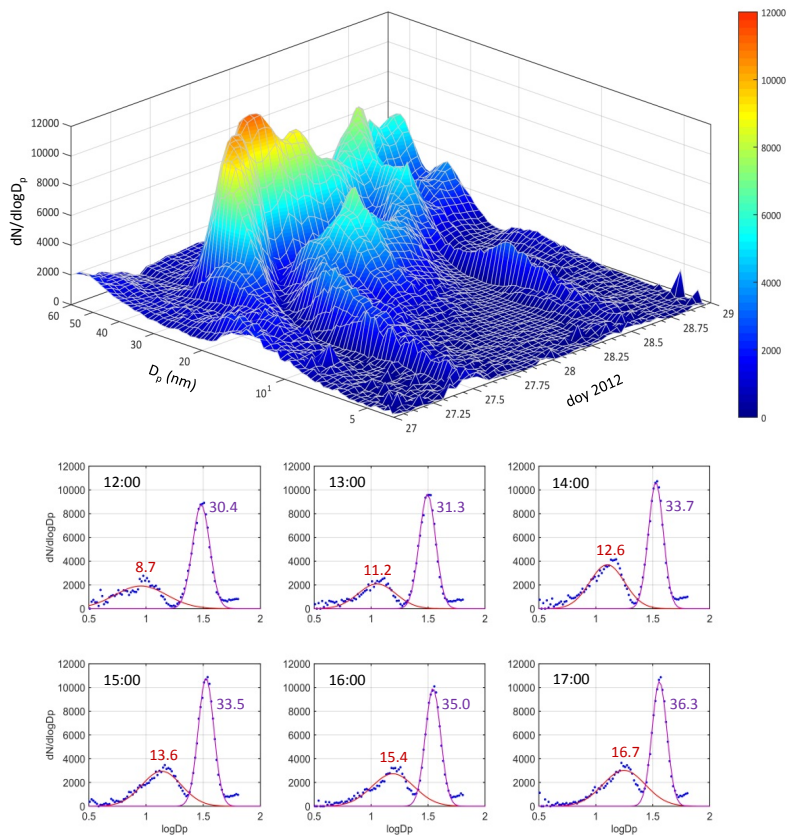
Figure 2. Detailed presentation of the NPF event around 27 January 2012 with a linear $dN/d\log D_p$ (cm^{-3}) scale as z axis, based on hourly mean SMPS data recorded with 64 channel resolution. The lower panel shows exemplarily six log-normal distribution fits through size distributions measured at 27 January between 12:00 and 17:00 UTC. The mode mean diameters (in nm) are noted next to the respecting modal maxima.
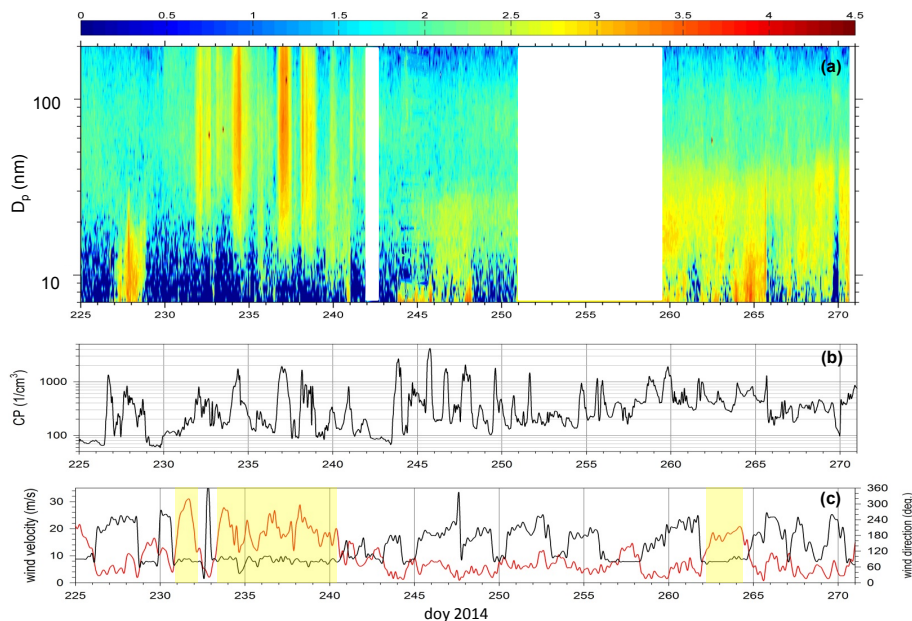
Figure 3. Time series of particle size distribution $dN/d\log D_p$ (cm^{-3}) measured during winter 2014 (12 August through 27 September, logarithmic color code to the right of the contour plot) **(a)**, CP concentration **(b)**, wind velocity (red line) and wind direction (black line) **(c)**. The yellowish shaded areas in **(c)** mark stormy weather conditions associated with snow drift.
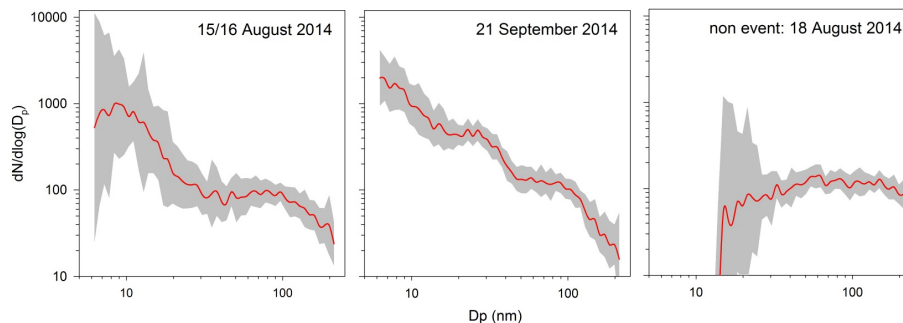
Figure 4. Mean size distribution (red line) and range of geometric standard deviation (grey envelope) during both winter particle nucleation events (15/16 August and 21 September 2014), as well as for typical winter day without nucleation (18 August 2012).